Hydrogen Adsorption in Potassium-Intercalated Graphite of Second Stage: An ab Initio Molecular Dynamics Study

Hansong Cheng,*,† Guido Pez,† Georg Kern,‡ Georg Kresse,‡ and Jürgen Hafner‡

Air Products and Chemicals, Inc., 7201 Hamilton Boulevard, Allentown, Pennsylvania 18195-1501, and Institut für Material Physik and Center for Computational Material Science, Universität Wien, Sensengasse 8, Wien, Austria

Received: June 13, 2000; In Final Form: November 15, 2000

We present an ab initio molecular dynamics study on hydrogen adsorption in potassium-intercalated graphite of second stage. The simulation utilizes the ultrasoft pseudopotenals plane wave method under local density functional approximation. The optimized lattice structures and the calculated H_2 adsorption energy are in excellent agreement with experiments. The simulation also well reproduces the previously observed lattice expansion due to H_2 uptake. The dynamics investigations reveal that not only the adsorbed hydrogen molecules but also the intercalated potassium atoms are highly mobile and assume a variety of two-dimensional configurations. The hydrogen dynamics is essentially chaotic within a layer of about 1.4 Å thickness centered between the graphite sheets, with a closest C−H distance of about 2.2 Å.

Introduction

Materials capable of storing hydrogen are of considerable fundamental and current practical interest, particularly in view of recent developments in fuel cell technologies.[1] Most investigated have been the metal hydride systems where the hydrogen is dissociatively bound;[2] but there have also been many studies on carbon and graphite-based sorbents where usually the binding is much weaker and the H_2 molecule remains intact.[3,4] Such a physisorption of H_2 is best demonstrated by the second-stage graphite intercalation compounds, $C_{24}M$ where M = K, Rb, and Cs, which at 77 °K adsorb up to two molecules of H_2 per formula unit.[5−9] Here the intercalated species including H_2 reside between the graphite planes with no intercalates between their nearest neighboring graphite sheets. The H_2 isosteric heat of adsorption at 63−90 °K for $C_{24}K$ is reported to be 2.21 and 2.7−3.0 or 2.0−2.17 kcal/mol depending on coverage and appears to be slightly higher for the cesium intercalate.[5−8] These are indicative of very weak interactions between hydrogen and the adsorbent but they are about twice as large as the isosteric heats of adsorption for hydrogen on graphitic carbons at zero coverage which range from 0.910 kcal/mol for *para*-hydrogen,[10] to 1.180 and 1.293 kcal/mol.[11,12] The corresponding heat for a high surface area porous carbon has been estimated to range from 1 to 1.25 kcal/mol, depending on coverage.[13] The apparently enhanced interaction of H_2 with the alkali metal−graphite systems has been described in terms of electronic charge-transfer effects.[14,15]

The structures of these graphite intercalation compounds (GIC) have been previously characterized by both theoretical and experimental studies.[16−20] Useful insight into the intercalating patterns has been gained by powder diffraction and neutron scattering techniques.[18] However, in general, reliable structural information could be obtained only along the *c*-axis and the 2-dimensional structure parallel to the graphite sheets could not be determined. The dynamic behavior of the intercalants and the detailed hydrogen adsorption mechanism are not well understood. Calculations using semiempirical quantum-mechanical methods[19] and Monte Carlo simulations[20] have provided useful information about the electronic structure and the in-plane structure of the compounds. In this paper, we present theoretical studies on hydrogen adsorption in stage-2 potassium intercalated graphite $C_{24}K$. The purpose of the present work is to better understand the structure and intercalant configurations upon hydrogen adsorption, and the energetics and overall mechanism of hydrogen uptake. The calculations were carried out using quantum mechanical ab initio molecular dynamics (MD) under the local density functional approximation (LDA).[21,22] The MD simulations allow us to determine where the potassium atoms are located and how hydrogen interacts with the intercalated material. The structures of the intercalated compound as well as the adsorption patterns were calculated and subsequently the adsorption energy was evaluated. Dynamic studies are used to analyze the liquidlike behavior of both the intercalated K atoms and the adsorbed H_2 molecules.

Computational Method

We utilized the Vienna Ab Initio Simulation Package (VASP) to carry out the calculations.[23,24] The computational method and procedure can be briefly described as follows: The electronic structure calculations were performed using a plane-wave basis set and optimized ultrasoft pseudopotentials with a cutoff energy E_{cut} = 290 eV in the local density approximation using the exchange-correlation functional proposed by Perdew and Zunger.[25−28] The ultra-soft pseudopotentials used for C and H have previously been tested extensively in calculations on bulk graphite and diamond, hydrocarbon molecules and H_2 adsorption on diamond as well as graphite surfaces.[29] For pure graphite the LDA yields lattice constants of a = 2.440 Å and c = 6.465 Å, in good agreement with experiment (a = 2.451 Å and c = 6.70 Å). The phonon dispersion relations for graphite have been calculated and found to be in excellent agreement with experi-

* Author to whom correspondence should be addressed.
† Air Products and Chemicals, Inc.
‡ Institut für Material Physik and Center for Computational Material Science.

10.1021/jp0021392 CCC: $20.00
Published on Web 12/21/2000

ment.[30] K was modeled by an ultra-soft pseudopotential that treats the 3p electrons as valence electrons for which the chosen cutoff energy is largely sufficient. The generalized Kohn−Sham equations were solved by employing an efficient band-by-band residual minimization procedure for the one-electron energies. The lattice structure optimization was performed with a quasi-Newton minimization algorithm. The MD simulations were performed in the canonical ensemble using the Nosé thermostat for temperature control.[31] The total energy is expressed as

$$E = \sum_i \frac{\mathbf{p}_i^2}{2m_i s^2} + \phi(\mathbf{q}) + \frac{p_s^2}{2Q} + gkT \ln s$$

where the first term is the kinetic energy, the second term is the free potential energy, the third term is the kinetic energy of the thermostat, and the fourth term is the potential energy of the thermostat. The forces acting on the atoms were calculated from the ground-state electronic energies according to the Hellmann−Feynman theorem at each time step and subsequently used in the integration of Newton's equation of motion. To speed up the dynamic simulations, the Brillouin zone was sampled only at the Γ-point, which was found sufficient to provide semiquantitative information on the H_2 adsorption energies. The mass of tritium was used for H, which allowed us to use a time step of 1 fs to simulate the dynamic system to 4 ps. It is understood that while the time-dependent properties such as diffusion rate will change accordingly, the time-independent behavior will remain the same. Finally, the temperature of 500 K was used throughout the MD simulations.

Results and Discussion

Unit Cell Structures. In the stage-2 $C_{24}K$ compound, the K atoms are intercalated between every second pair of honeycomb-like layer of C atoms stacked in an *AB* sequence such that the atoms in the *B*-layers lie above the centers of the hexagonal rings in the *A*-layer. The intercalation expands the interlayer distance from 3.35 Å to 5.40 Å, while the distance between layers with no intercalates remains almost unaffected. The structure of this compound is only precisely known with respect to the graphite interlayer spacings; the specific locations of the potassium atoms are not well defined, although some rough estimate of the K−K distances has been reported.[32] A slight lattice expansion upon H_2 adsorption is also noted.

To facilitate the MD simulation, we chose a unit cell of the K-intercalated material that contains 48 C and 2 K atoms, which accommodates 4 H_2 molecules. Simulation on a larger unit cell was also performed for a shorter period of time, which gives qualitatively similar results as will be shown later in this article. Figure 1 displays the selected unit cell of the Bravais lattice of the compound as defined by

$$\mathbf{a} = (a,0,0)$$

$$\mathbf{b} = \left(\frac{1}{2}a,\frac{\sqrt{3}}{2}a,0\right)$$

$$\mathbf{c} = \left(\frac{1}{6}a,0,c\right)$$

The unit cell includes two layers of graphite sheets and one layer of the intercalants. It is large enough to allow all atoms to move freely without encountering significant lattice symmetry constraints. The cell parameters, *a* and *c*, together with all atomic coordinates, were optimized for a given configuration at both the presence and absence of H_2.

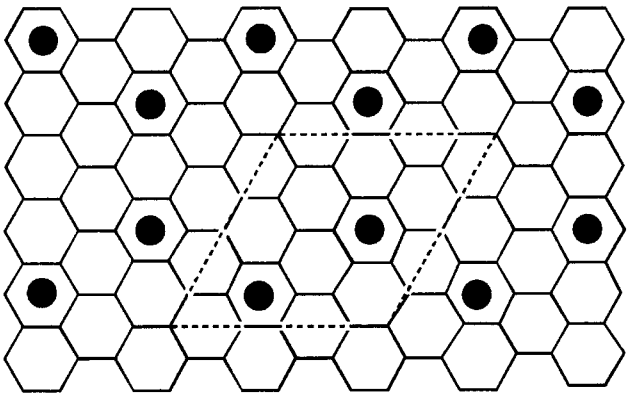

Figure 1. Unit cell used in our MD simulation. It includes two layers of graphite sheets and one layer of intercalants. The unit cell contains 50 atoms for $C_{24}K$ and 58 atoms for $C_{24}K{\cdot}H_2$. The second layer of graphite is not shown here. The dots represent the K atoms in the starting configuration. For $C_{24}K$, the intercalant layer contains two K atoms; upon H_2 adsorption, it also includes 4 hydrogen molecules.

TABLE 1: Optimized and Experimentally Available Cell Parameters (unit: Å)

	C_{24K}		$C_{24}K{\cdot}H_2$	
cell parameter	calcd	expt[a]	calcd	expt[a]
a	8.497		8.497	
c	8.413	8.75	8.829	9.04

[a] The experimental values were obtained under the assumption that the distance between the graphite layers containing no intercalates is the same as the one in pure graphite (3.35 Å).

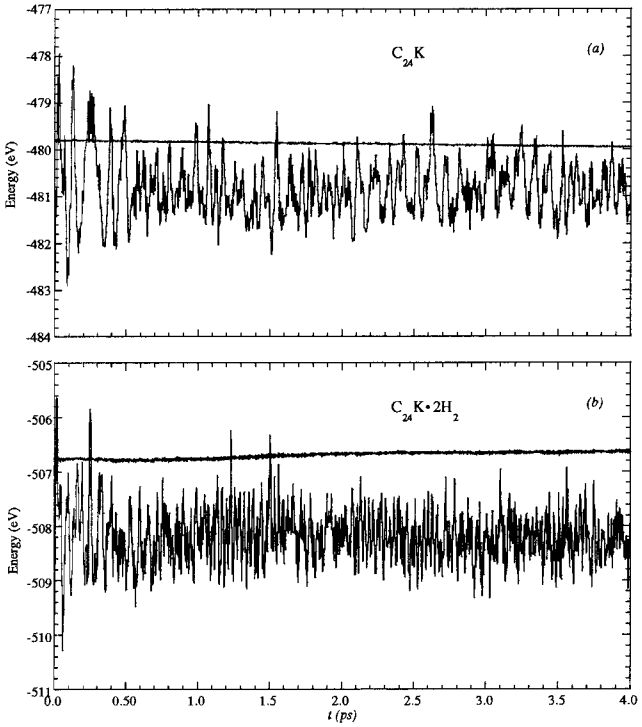

Figure 2. Time evolution of total potential energy for $C_{24}K$ (a) and $C_{24}K{\cdot}H_2$ (b). The straight line represents the total energy.

The optimized cell parameters as well as the available experimental values are shown in Table 1. While the cell vectors parallel to the graphite plane remain essentially unchanged, the lattice expands slightly with the lattice spacing between the

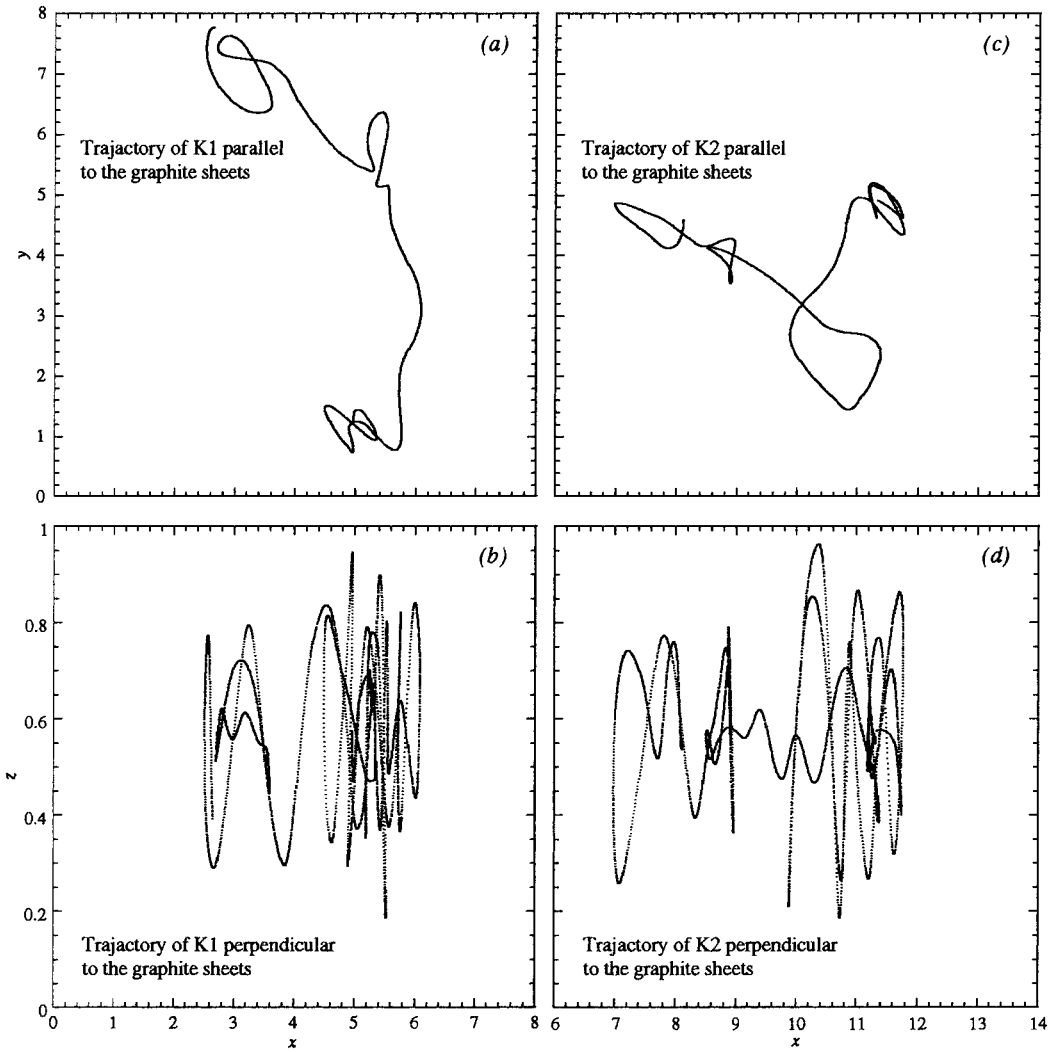

Figure 3. The calculated trajectories of the two K atoms in the unit cell. Here (a) and (c) record their *x*, *y* coordinates while (b) and (d) collect their *x*, *z* coordinates.

graphite sheets containing the intercalants changing from 5.284 to 5.694 Å upon H_2 adsorption, in good agreement with the previous experimental observation (from 5.40 Å to 5.69 Å).[2] We subsequently fixed the cell parameters and utilized the fully optimized structures as the starting configurations in our MD simulations.

It must be stressed that real fluid structure cannot be simply characterized by using only a few intercalating atoms. The present study is to address the issue of high diffusivity of these species in the GICs and to compare it with their high mobility observed in experiments. Simulation on a relatively small unit cell allows us to gain useful insight into the fluidlike behavior of these species.

Adsorption Energetics. The calculated time evolution of total potential energies with the absence and presence of H_2 is shown in Figure 2. The averaged total potential energies of $C_{24}K$ and $C_{24}K{\cdot}H_2$ starting from 1 ps are −480.868 eV and −508.193 eV, respectively. The estimated uncertainty of the energy average is approximately ±0.05 eV. Furthermore, the LDA calculation gives a total potential energy of −6.677 eV for the free H_2 molecule. We thus obtained the H_2 adsorption energy in $C_{24}K$ of −3.60 kcal/mol, in good agreement with the reported experimental heat of adsorption (−2.3 kcal/mol). We note that although LDA is known to be overbinding, the error is largely canceled out when evaluating the relative energy differences in the MD simulation.

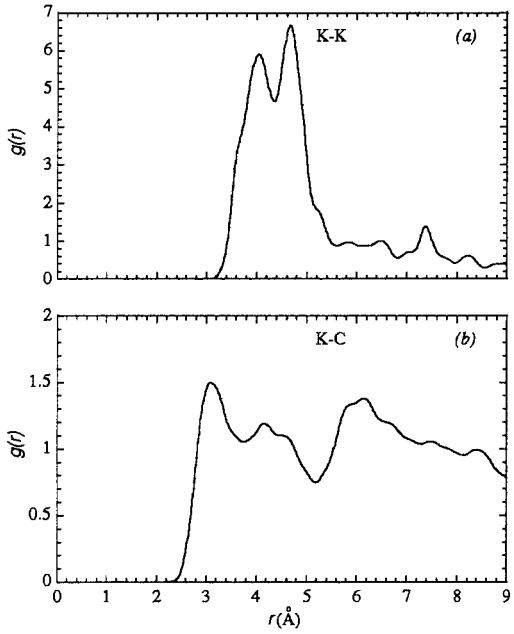

Figure 4. Radial distribution function of K−K and K−C distances in $C_{24}K$: K−K (a) and K−C (b).

It should be pointed out that the small change in H_2 adsorption energy energies is well within the uncertainty of the theoretical

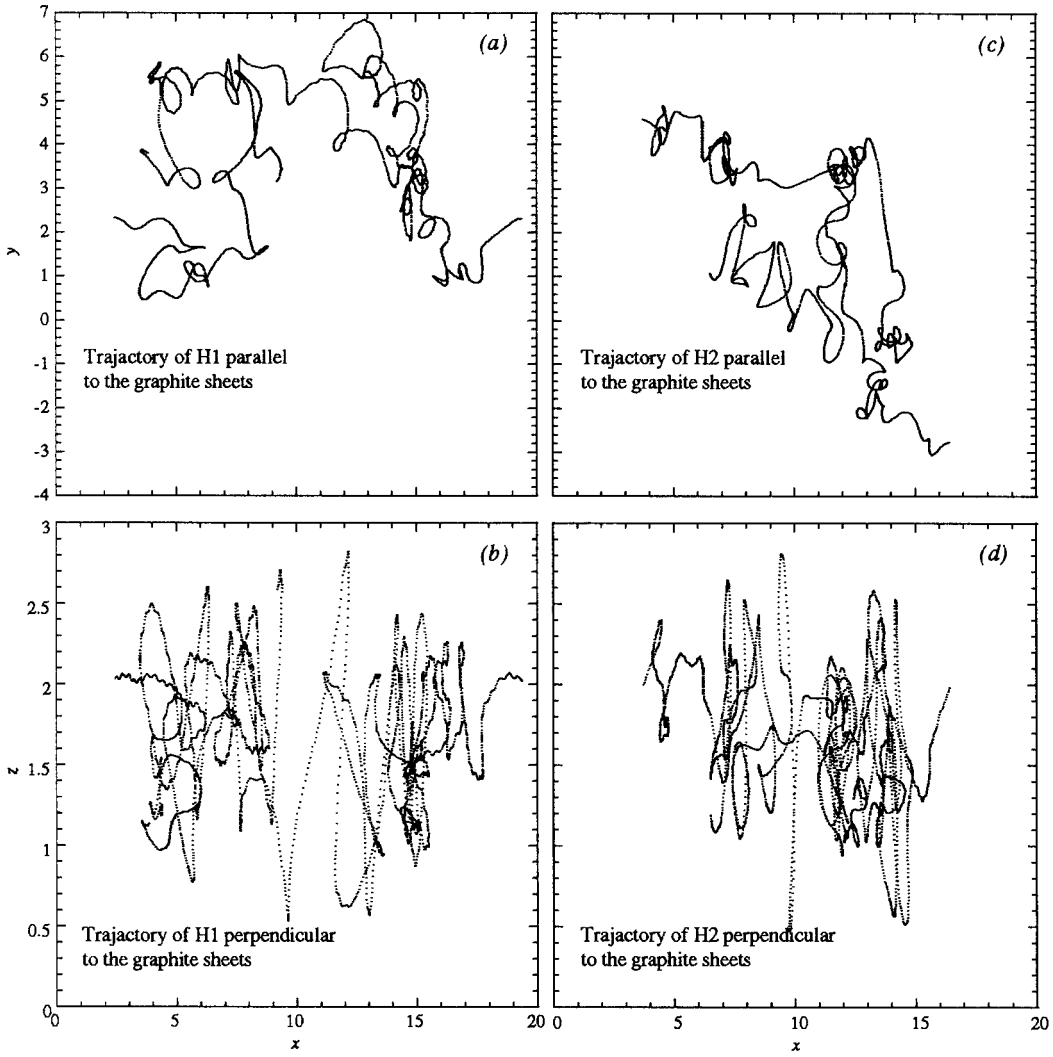

Figure 5. The calculated trajectories of the two selected H atoms in the unit cell of $C_{24}K{\cdot}H_2$. Here (a) and (c) record their *x*, *y* coordinates while (b) and (d) collect their *x*, *z* coordinates.

method used in this study, even though the trend predicted in the theoretical calculation is consistent with the experiments. However, the semiquantitative results together with the analysis on the dynamics and electronic properties of the GIC system provide useful insight into the role of the intercalating metals in the H_2 adsorption.

Trajectory Analysis. From the calculated trajectory, we found that the metal atoms in general do not reside at specific sites but instead move around like a flow between the graphite sheets. To show their dynamic behavior, we display the fluid trajectories of the two potassium atoms in the unit cell in Figure 3, where parts a and c record their *x*, *y* coordinates while parts b and d collect their *x*, *z* coordinates. Figure 3, parts a and c, project the trajectories of the two atoms on a plane parallel to the graphite sheets, which clearly shows that the potassium atoms are capable of floating around over the entire unit cell while the graphite sheets remain essentially still at their relative positions. Figure 3, parts b and d, yield information on the dynamic behavior of the potassium atoms in the direction perpendicular to the graphite plane. They indicate that the atoms move up and down rapidly between the graphite sheets over a range of up to ±0.4 Å in concert with the movement of the carbon atoms of graphite which exhibit considerable elasticity in the dynamic process. At the chosen temperature the maximum displacement of the carbon atoms in the direction perpendicular to the graphite layers is about 0.28 Å. None of the metal atoms was found to be associated with any particular site or atom in the graphite sheets. Their trajectories in the lattice are essentially chaotic. The simulated dynamic behavior of potassium is qualitatively consistent with the experimental observation that the atoms behave like a fluid in the lattice, which made the X-ray diffraction techniques incapable of resolving the 2-D structure.

Figure 4 displays the radial distribution function for the K−K and K−C distances, where the latter yields information about the distance of K from the graphite wall. Although the K−K distance changes dynamically, it is largely concentrated in two regions. The first one is around 4 Å. Our LDA calculation for a gas-phase potassium dimer gives a bond distance of 3.844 Å. This seems to suggest that a considerable amount of potassium atoms in the superlattice have an interatomic distance slightly longer than that of dimers. The two potassium atoms are loosely tied together, and are readily falling apart. In the second region, the calculated K−K distance is approximately 4.7 Å, significantly higher than the dimer bond length. This is the region where the potassium atoms are most evenly distributed. The potassium atoms exhibit various configurations. Some of the well-aligned distribution pattern is likely attributed to the periodic boundary condition and the relatively small unit cell used in our simulation. In fact, when a larger unit cell was used, the distribution configurations of the potassium atoms become more complicated. Nevertheless, the K−K distances are still

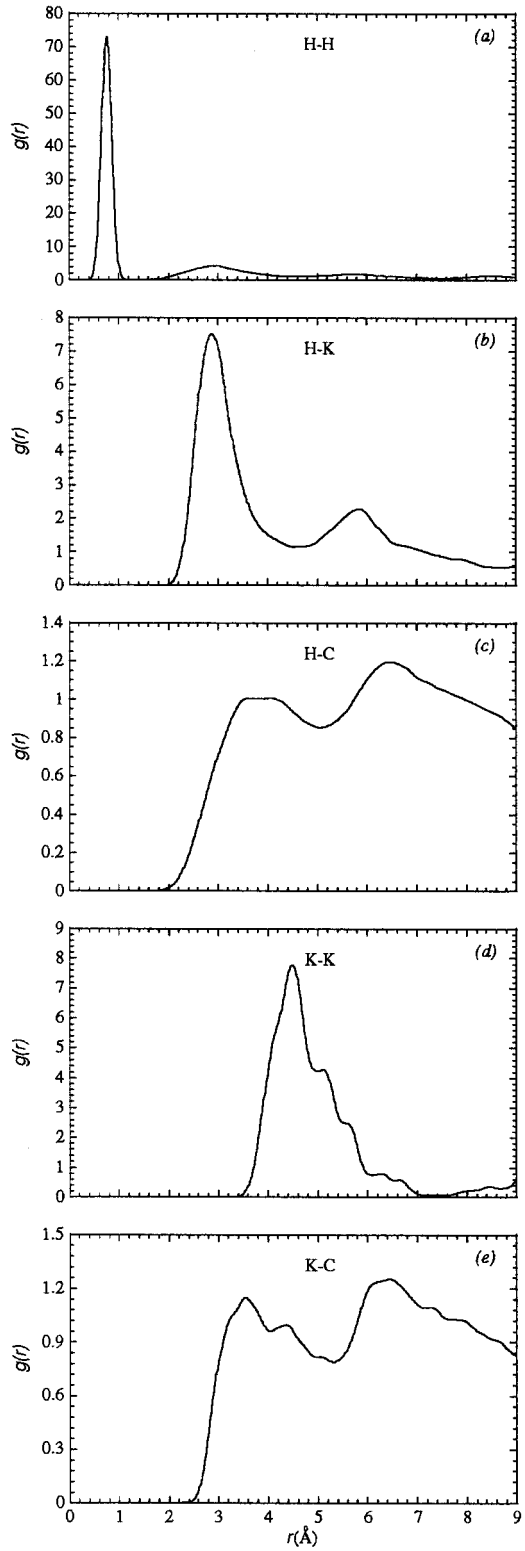

Figure 6. Radial distribution function of the key bond parameters in $C_{24}K{\cdot}H_2$. (a) H−H. (b) H−K. (c) H−C. (d) K−K. (e) K−C.

populated mostly in these two regions. The closest K−C distance in our simulation is around 3 Å, indicating that the potassium atoms are in close contact with the graphite sheets. Finally, we note that the graphite sheets slide slightly in the dynamic process with individual carbon atoms moving up and down, allowing dynamic access by H_2.

The trajectories of the potassium atoms upon hydrogen adsorption are similar to the ones shown in Figure 3. The dynamic trajectories of selected two separated hydrogen atoms

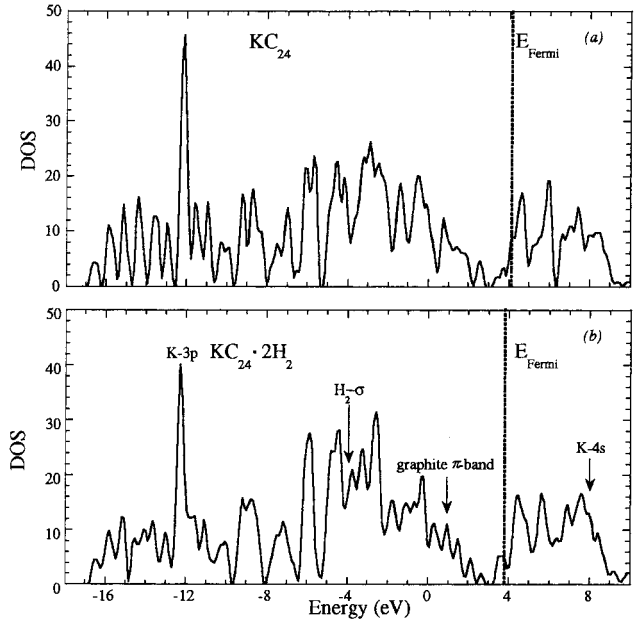

Figure 7. The typical calculated density of states for the selected configurations of $C_{24}K$ and $C_{24}K{\cdot}H_2$ in the MD process. (a) and (b) are for $C_{24}K$ and $C_{24}K{\cdot}H_2$, respectively.

in $KC_{24}{\cdot}H_2$ are depicted in Figure 5. For each of atoms the trajectory of the other atom in the hydrogen molecule exhibits similar features. Since the molecular H_2 bond is never broken, these trajectories also reflect the movement of the entire molecule. The H_2 molecules appear to be moving much faster than the potassium atoms due to their smaller mass. In principle, for light atoms such as hydrogen the quantum nature of the dynamics cannot be ignored. For H_2 molecules moving on a fixed potential energy surface, quantum simulations of the dynamics have been performed.[33] In the present case, however, the effective potential energy surface on which the H_2 molecules move changes at every moment due to the rapid dynamics of the K atoms and of the C layers. For the coupled sorbent−adsorbate system a quantum simulation is feasible with path integral methods (e.g., ref 34); however, these are computationally very expensive at present. It is seen from the trajectories that like potassium atoms, the hydrogen molecules are not attached to any specific atom or site. Instead, they float around over the intercalated layers rapidly, actively interacting with both potassium atoms and graphite sheets. Because of their relatively small size, the H_2 molecules are capable of moving up and down in a wider range than the potassium atoms.

The calculated radial distribution function of several key geometric parameters in $KC_{24}{\cdot}H_2$ is shown in Figure 6. While the H−H distance in the H_2 molecule remains around 0.8 Å, the intermolecular distance spans approximately from 2.5 Å to 4.5 Å. The H_2 bond distance can stretch from the optimized value in the absence of graphite (0.7649 Å) by about 0.1−0.2 Å. The H−K distance can be as short as 2.5 Å and is peaked at 3.0 Å. At a short H−K distance the H_2 molecule is side-on to the potassium atom, while the effect of H_2 orientation on the energetics is insignificant at large H−K separations. The radial distribution function of the H−C distance suggests that H_2 molecules can also weakly interact with the graphite walls as they approach the carbon atoms. The minimum interaction distance is about 2.055 Å with the orientation of H_2 molecule being head-on to the graphite carbon. Comparing with Figure 4, one sees that the peak position of the K−K nearest neighbor distance is shifted from 4.0 Å to about 4.4 Å upon H_2 adsorption, indicating the influence of the adsorption on the arrangement

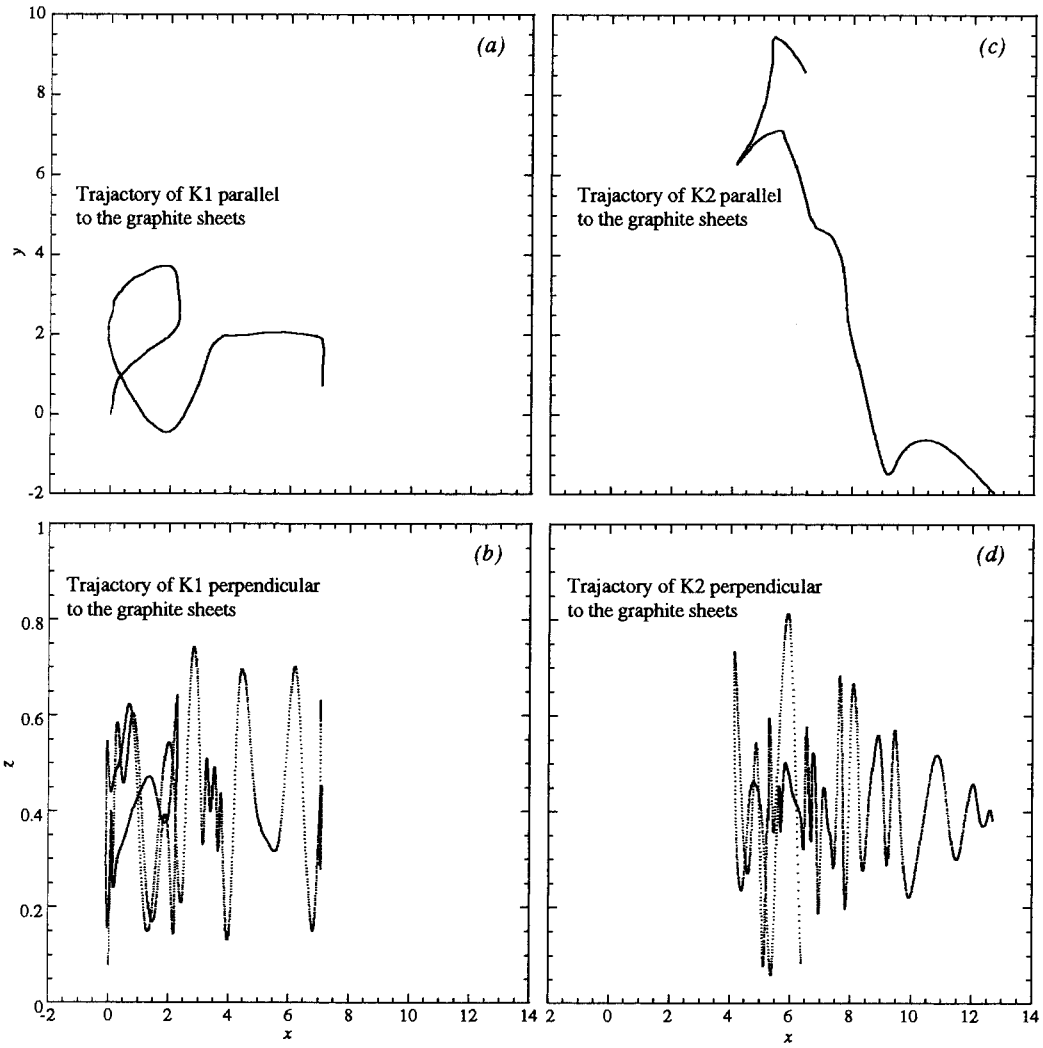

Figure 8. The calculated trajectories of the two selected K atoms in the rectangular cell of $C_{24}K$. Here (a) and (c) record their *x, y* coordinates while (b) and (d) collect their *x, z* coordinates.

of the intercalating atoms. The distribution of the K−C distances essentially remains the same as in KC_{24}, as expected.

Density of States. We chose a typical configuration near the equilibrium to show the calculated density of states spectrum (DOS). The DOS spectra for other configurations upon reaching equilibrium exhibit similar features, although the detailed structures may vary accordingly. Figure 7 shows the DOS spectra of KC_{24} and $KC_{24}{\cdot}2H_2$, respectively, where some of the key features of the energy bands are highlighted. The highest occupied states are primarily of graphite π character and the potassium 4s band is well above the Fermi level, leading to an electron transfer to the graphite's π^* band. This results in a metallic character of the intercalation compound. On the other hand, the σ^* band of H_2 overlaps well with the 4s band of K. Their orbital symmetries match each other nicely with an orientation of H_2 side-on to the K atom. The σ^* band of H_2 resides only slightly above the Fermi level. This allows H_2 to compete with the graphite π^* band for the 4s electron from K, which gives rise to the adsorption of H_2 in the material. As a consequence, the Fermi level shifts slightly downward.

Unit Cell Size Effect. Admittedly, the unit cell used in our ab initio MD simulation is relatively small. As a consequence, the present approach may not adequately describe the fluidlike behavior of the intercalated species as observed in experiments due to the small number of intercalants used in the unit cell. Computationally, it would be prohibitively impractical to include a large number of intercalants with the correct chemical composition required to represent the fluids in the ab initio MD simulation. Instead, we choose a unit cell twice as large as the one used in our simulation to investigate the effect of the unit cell size on the simulation results since the goal of the present work is to gain qualitative understanding on the interplay between the intercalants and the graphite layers. For purpose of comparison, we choose a rectangular cell that contains 4 K atoms, 8 H_2 molecules, and 2 layers of graphite sheets with 48 C atoms on each. The optimized cell parameters are $a = 8.496$ Å, $b = 14.718$ Å, and $c = 8.296$ Å, respectively, with potassium as the only intercalating species. The *c*-axis expands by 0.419 Å upon H_2 adsorption while the other cell parameters remain unchanged. The MD simulation time for KC_{24} was 3.5 ps and only 1.5 ps for $KC_{24}{\cdot}H_2$ due to the computational cost.

The estimated H_2 adsorption energy is −4.69 kcal/mol, slightly above the one calculated with the smaller unit cell, partly because of the short simulation time. Figure 8 displays the trajectories of two of the K atoms in the unit cell prior to H_2 adsorption. Other K atoms exhibit a similar trajectory pattern. Similar to the situation of smaller cell, the intercalants are not bound up with specific sites of the graphite planes. Instead, they move around over the entire unit cell within 3 ps, resembling the fluidlike behavior. The calculated radial distribution functions also exhibit qualitatively similar features to those shown in Figures 4 and 6, except the relative magnitudes differ slightly.

The source of the differences is likely due to the insufficient statistics of the simulation resulting from the relatively short simulation time.

In general, we find that size of the unit cell does not significantly affect the qualitative results of the simulation for the KC_{24} compound.

Summary

There have been many experimental studies on the potential applications of the alkali metal−intercalated graphite compounds for hydrogen storage with little understanding of the detailed adsorption mechanism. Our ab initio MD simulation is the first attempt to gain insight into the dynamic behavior of both intercalate atoms and adsorbed molecules in the second stage potassium-intercalated graphite compound and yields useful information on the adsorption energetics. First, we found that the intercalated potassium atoms do not exhibit a specific distribution pattern in the lattice; instead, the distribution changes with time. The potassium atoms "float" around over the lattice without attaching themselves to any specific sites of graphite sheets. The calculated radial distribution function shows that the most prominent K−K distance in the lattice is slightly above the value found for the gas-phase potassium dimers and, upon H_2 adsorption, its peak position in the radial distribution function shifts up further by about 0.4 Å, as a result of the influence of H_2 molecules. This simulated dynamic picture is consistent with the experimental observations. Second, we found numerous adsorption sites for H_2 with comparable energetics. Like potassium, the hydrogen molecules can readily float around in the lattice to interact with both potassium and graphite with specific orientations; however, their movement is much faster due to their smaller mass. Again, no specific site preference was found for hydrogen to attach to either the graphite layers or to the intercalant layers. Finally, our LDA calculation yields the optimized cell parameters in good agreement with the experimental values. In particular, the lattice expansion due to H_2 adsorption observed in experiment was nicely reproduced. The calculated H_2 adsorption energy was in good agreement with the experimental enthalpy of H_2 adsorption. The MD simulation results presented in this paper were obtained by sampling the Brillouin zone only at the Γ-point. Numerical tests with a $2 \times 2 \times 1$ grid shows no significant change in the final results. Due to the relatively small unit cell used in our simulation, it is difficult to apply the classical diffusion theory to the current work to derive the diffusion coefficients for lack of sufficient statistics. Nevertheless, we have demonstrated in this paper that the present method is capable of providing reliable quantitative or semiquantitative information about the structure, energetics, and dynamics of hydrogen adsorption in the $C_{24}K$ prototypical graphite intercalated compound.

Acknowledgment. H.C. is very grateful to Professor Hafner and his research group for their hospitality during his short visit to Vienna where part of this work was carried out. The authors also express their gratitude to Dr. J. Higgins for providing the initial structure KC_{24} structure coordinates and to Drs. B. Peterson, A. Cooper, and S. Mayorga for many useful discussions. The support by Drs. C. Valenzuela and J. Pfeiffer (Air Products) is also gratefully acknowledged.

References and Notes

(1) Ralph, T.; Hards, G. *Chem. Ind.* **1998**, 337.

(2) Verbetsky, V.; Malyshenko, S.; Mitrokhin, S.; Solovei, V.; Shmal'ko, Y. *Int. J. Hydrogen Energy* **1998**, *23*, 1165.

(3) Noh, J.; Agarwal, K.; Schwarz, J. *Int. J. Hydrogen Energy* **1987**, *12*, 693.

(4) Terai, T.; Takahashi, Y. *Mater. Sci. Forum* **1992**, *91*, 839.

(5) Watanabe, K.; Soma, M.; Onishi, T.; Tamaru, K. *Nature* **1971**, *233*, 160.

(6) Watanabe, K.; Kondow, T.; Soma, M.; Onishi, T.; Tamaru, K. *Proc. R. Soc. London* **1973**, *A333*, 51.

(7) Lagrange, P.; Metrot, A.; Herold, A. *C. R. Acad. Sci. Ser.* **1972**, *C275*, 765.

(8) Terai, T.; Takahashi, Y. *Synth. Met.* **1989**, *34*, 329; Watanabe, K.; Kondow, T.; Onishi, T.; Tamaru, K. *Chem. Lett.* **1972**, 477.

(9) Murakami, H.; Kanazawa, I.; Sano, M.; Enoki, T.; Inokuchi, H. *Synth. Met.* **1989**, *32*, 135.

(10) Pace, E.; Siebert, A. *J. Phys. Chem.* **1959**, *63*, 1398.

(11) Dericbourg, J. *Surf. Sci.* **1976**, *59*, 565.

(12) Constabaris, G.; Sams, J.; Halsey, G. *J. Phys. Chem.* **1961**, *65*, 367.

(13) Pez, G.; Steyert, W. *U.S. Patent 4*, **1986**, *580*, 404.

(14) Yea, N.; Enoki, T.; Salamanca-Riba, L.; Dresselhaus, G. *Mater. Res. Soc.* **1986**, *56*, 467.

(15) Doll, G.; Eklund, P. C.; Senatore, G. In *Intercalation Layered Materials*, NATO ASI Ser. **1986**, *B148*, 309.

(16) Foley, G. M. T.; Fischer, J. E. *Phys. Rev. B.* **1979**, 6474.

(17) Parry, G. S. *Mater. Sci. Eng.* **1977**, *31*, 99.

(18) Clarke, R.; Caswell, N.; Solin, S. A.; Horn, P. M. *Physica B* **1980**, *99*, 457.

(19) Böhm, M. C.; Schulte, J.; Schlögl, R. *Phys. Status Solidi B* **1996**, *196*, 131.

(20) Arai, A.; Shirakawa, Y.; Tamaki, S. *J. Non-Cryst. Solids* **1996**, *205*, 803.

(21) Dahl, J.; Avery, A. *Local Density Approximations in Quantum Chemistry and Solid State Physics*; Plenum, New York,1985.

(22) Jones, R. O.; Gunnarsson, O. *Rev. Mod. Phys.* **1989**, *61*, 689.

(23) Kresse, G.; Hafner, J. *Phys. Rev. B* **1993**, *47*, 558; *ibid.* **1994**, *49*, 14251.

(24) Kresse, G.; Furthmüller, J. *Comput. Mater. Sci.* ***1996***, *6*, 15; *Phys. Rev. B* **1996**, *55*, 11169.

(25) Vanderbilt, D. *Phys. Rev. B* **1990**, *41*, 7892.

(26) Laasonen, K.; Pasquarello, A.; Car, R.; Lee, C.; Vanderbilt, D. *Phys. Rev. B* **1992**, *47*, 10142.

(27) Kresse G.; Hafner, J. *J. Phys.: Condens. Matter* **1994**, *6*, 8245.

(28) Perdew, J.; Zunger, A. *Phys. Rev. B* **1981**, *23*, 5048.

(29) Kern, G.; Hafner, J.; Kress, G. *Surf. Sci.* **1996**, *366*, 445; Kern, G.; Hafner, J. *Phys. Rev. B* **1997**, *56*, 4203.

(30) Kresse, G.; Furthmüller, J.; Hafner, J. *Europhys. Lett.* **1995**, *32*, 729.

(31) Nosé, S. *J. Chem. Phys.* **1984**, *81*, 511.

(32) Zabel, H.; Jan, Y. M.; Moss, S. C. *Physica* **1980**, *99B*, 453.

(33) Gross, A.; Wilke, S.; Scheffler, M. *Phys. Rev. Lett.* **1995**, *75*, 2718.

(34) Marx D.; Parrinello, M. *Science* **1996**, *271*, 179.